A Consideration on the Energy Efficiency of Agitation in Emulsion

Hisao HIDAKA, Shun'ichi NORO*, Akira TAKAMURA,* and Masumi KOISHI**

Department of Science and Engineering, Meisei University, Hodokubo, Hino-shi, Tokyo 191
**Meiji College of Pharmacy, Yato-cho, Tanashi-shi, Tokyo 188*
***Faculty of Pharmaceutical Science, Science University of Tokyo, Ichigaya Funakawara-machi, Shinjuku-ku, Tokyo 162*

(Received June 9, 1976)

The effects of mechanical factors on the energy efficieucy of agitation in o/w-type emulsions were investigated. The impeller diameters used were 49.0, 65.0, 80.1, and 89.9 mmϕ and the number of revolution was set at 200, 330, 400, 530, 660, or 812 rpm. The viscosity ratios (μ_d/μ_c) were 0.836: 1, 0.0861: 1, 0.000777: 1, and 0.000173: 1. The size of the dispersed liquid droplets was measured by the microphotographic method. The mean diameter of the droplets, their size distribution, and the agitation torque were determined, and the energy efficiency of agitation was evaluated. When the viscosity ratio was near 0.00861: 1, the energy efficiency of agitation showed a maximum. Furthermore, the energy efficiency decreased as the mean surface-volume diameter became smaller.

Agitation is one of the most important factors affecting the formation of emulsions when a specific emulsification method and specific emulsifying equipment are used:[1,2] more efficient agitation gives better emulsions. Now, the energy consumption related to agitation is considered to be due not only to the creation of new interfaces but also to setting the liquid in motion against viscous resistance in an emulsifying machine.[3,4] That is, the required input power of an agitator will depend upon various factors,[5] so it is very difficult to give a complete theoretical formula for agitation power. Even if the flow pattern is unknown, however, the relationship between agitation power and many mechanical factors may be formulated by the method of dimensional analysis, if the latter can be expressed in terms of such physical parameters as the diameter of the impeller and its rate of revolution.[6]

In this study, therefore, agitation power is first calculated from the torque value[7] and then the agitation energy[8] is evaluated as the product of agitation power and agitation time in the case of a liquid-liquid dispersion.[9] Secondly, the total interfacial energy of the emulsion is calculated as the product of the interfacial area and the interfacial tension.[8] The interfacial area is considered to be the most important factor[10] in the formation of emulsions and it is strongly affected by mechanical stirring. If the total interfacial energy and the agitation energy are calculated, the energy efficiency of agitation is then defined as the ratio of these two quantities.[8]

In this paper, therefore, the energy efficiency of agitation in the emulsion formation will be experimentally examined in relation to the impeller diameter, the revolution number, agitation torque, agitation power, the mean diameter of the dispersed phase, and interfacial tension.

Experimental

Equipment. The apparatus employed was the same one as described in our previous report.[11] The clear acrylate resin agitation tanks with 4 baffles were 150—200 mmϕ in diameter and 120—200 mm in depth. The stainless-steel agitation impeller (49.0—89.8 mmϕ) was of the standard Rushton-type with 6 blades. The tank was surrounded by a water jacket in order to keep the temperature of the liquid in it at 20.0 °C. The values of the tank diameter, the impeller diameter, and the number of revolution are summarized in Table 1.

TABLE 1. VALUES OF D_T, D_h, D_I, D_A, AND D_B OF THE APPARATUS EMPLOYED AND OF THE REVOLUTION NUMBER USED IN AGITATION

Tank size		Impeller size			Revolution number
D_T (mm)	D_h (mm)	D_I (mm)	D_A (mm)	D_B (mm)	N (rpm)
150	120	49.0	13.3	9.5	200, 330, 400,
		65.0	17.0	12.9	530, 660, 812
		80.1	19.9	15.9	
		89.8	24.9	17.1	
200	160	49.0	13.3	9.5	200, 330, 400,
		65.0	17.0	12.9	530, 660, 812
		80.1	19.9	15.9	
		89.8	24.9	17.1	
250	200	49.0	13.3	9.5	200, 330, 400,
		65.0	17.0	12.9	530, 660, 812
		80.1	19.9	15.9	
		89.8	24.9	17.1	

Measurement of Agitation Torque. The rotary torque meter used was of the Yamazaki SS-IR type (Yamazaki Seiki Laboratories) and was equipped with a stroboscope of the Sugawara PS-240 type (Sugawara Laboratory). The torque meter was tightly bound to the middle of the rotary shaft of the agitator, to prevent any precessional motion. Shortly after a liquid-liquid dispersion was formed, the torque was directly read with the light beam the stroboscope, which was exactly synchronized with the revolution of the impeller.

Measurement of Physical Properties. Mixtures of sodium silicate (Kishida Chemical Co.) and distilled water in varying ratios were used as the continuous phase. The total concentration of sodium silicate in the mixture ranged from 52.0 to 96.3% (w/w). The dispersed phase was made by mixing n-C_7H_{16} and CCl_4 in various volume ratios; the density was adjusted so as to be the same as that of the continuous phase (1.000—1.610 g/cm^3). Tween-20 (Tōhō Chemical Industry Co.) was employed as the emulsifying agent; its concentration was 0.1% (w/w). Interfacial tensions were measured by the ring method, and the viscosities of the liquid were measured by a rotating viscometer at 20.0±0.1 °C. The viscosity ratio, μ_d/μ_c, was widely varied, from 0.836: 1 to 0.000173: 1. The concentration of sodium silicate, the density of the continuous phase, the density ratio, the viscosity of the continuous phase,

TABLE 2. PHYSICAL PROPERTIES OF EACH CONTINUOUS PHASE

Concentration of sodium silicate (%, w/w)	Concentration of Tween-20 (%, w/w)	Density of continuous phase ρ_c (g/cm^3)	Density ratio ρ_d/ρ_c (—)	Viscosity of continuous phase μ_c (g/cm s)	Viscosity ratio μ_d/μ_c (—)	Interfacial tension $\lvert\gamma_d-\gamma_c\rvert$ (dyn/cm)
0.0	0.1	1.000	1.000	1.005	0.836	22.85
52.0	0.1	1.317	1.000	9.755	8.61×10^{-2}	15.62
75.0	0.1	1.486	1.000	97.60	8.61×10^{-3}	19.00
88.0	0.1	1.560	1.000	1082.0	7.77×10^{-4}	21.58
96.3	0.1	1.610	1.000	4860.0	1.73×10^{-4}	22.00

the viscosity ratio, and the interfacial tension are summarized in Table 2.

Experimental Procedure. The experiments were carried out under the following conditions:

(1) The viscosity ratios, μ_d/μ_c, used were 0.836: 1, 0.0861: 1, 0.00861: 1, 0.000777: 1, and 0.000173: 1.

(2) The tank diameters were 150, 200, and 250 mmϕ.

(3) The impeller diameters were 49.0, 65.0, 80.1, and 89.8 mmϕ.

(4) The revolution numbers of 200, 330, 400, 530, 660, and 812 rpm were employed.

The agitation tank was filled with 1960 ml of an aqueous sodium silicate solution, the continuous phase, containing Tween-20 as an emulsifying agent. The impeller was set at the center of the tank. In the middle of the impeller were gently placed 40 ml of a mixed solvent, the dispersed phase, to form a spherical drop.

The concentration of the dispersed phase was kept at 2.0% (w/w). Sixty minutes after agitation started, the liquid was sampled with a glass tube (5 mmϕ).

Each sample was photographed with a Nikon AFM camera equipped with a microscope. The diameters of the droplets were measured with a micrometer scale which had been photographed and enlarged under the same conditions. The number of droplets measured was one thousand in all cases. The mean length diameter, the mean surface diameter, the mean volume diameter, the standard deviation, and the particle size distribution were calculated by means of a Seiko-301 computer.

Calculation of Agitation Torque and Agitation Energy. The agitation power, P, can generally be represented, as shown below, by a function of the impeller diameter (D_I), revolution number (N), density of continuous phase (ρ_c), and viscosity of continuous phase (μ_c), when the dimensional analysis is applied to the case of turbulent flow.[12]

$$P = N_p(\rho_c N^3 D_I^5) \tag{1}$$

Here N_p is called the power number and is a function of impeller shape and Reynolds number.[13]

When the angular velocity of the impeller and the agitation torque are ω (rad/s) and T (kgw m), respectively, the agitation power P (kgw m/s) can be written as:

$$P = \omega T \tag{2}$$

Since the angular velocity is given by

$$\omega = 2\pi N \tag{3}$$

the agitation power can be written as:

$$\omega = 2\pi NT \tag{4}$$

Accordingly, if the agitation torque and the revolution number are exactly measured, the agitation power can be evaluated from Eq. 4.

When the agitation power is expressed in watts, the agitation energy E_A is given as the product of agitation power P and agitation time θ:

$$E_A = P\theta \tag{5}$$

Combining Eqs. 4 and 5,

$$E_A = 2\pi NT\theta \tag{6}$$

Consequently, the agitation energy can be obtained explicitly from Eq. 6.

Determination of the Energy Efficiency of Agitation. When the total interfacial area of the emulsion increases from S_1 to S_2, the increase in the total interfacial energy is calculated by the following equation:

$$E_s = \gamma(S_2-S_1) = \frac{6\gamma}{\rho_d}\left(\frac{1}{d_{sv_2}}-\frac{1}{d_{sv_1}}\right) \tag{7}$$

In order to investigate to what extent the agitation energy affects the increase in the total interfacial energy, the energy efficiency of agitation is defined as:

$$\eta = \frac{E_s}{E_A} = \frac{\gamma(S_2-S_1)}{P\theta} \tag{8}$$

Equation 8 gives the ratio of the total interfacial energy to the agitation energy, this is named the energy efficiency of agitation in mechanical dispersion. If the energy efficiency can be calculated under a certain agitation condition, it will be very useful for the research which looks for the optimum physical and mechanical conditions to obtain a good emulsion.

Results and Discussion

Relationship between Agitation Torque and Agitation Intensity. Agitation torques were measured at various impeller sizes and revolution numbers for two tank diameters, under a constant viscosity ratio in the range of μ_d/μ_c=0.836: 1—0.000173: 1. Figure 1 gives the relation between the agitation torque and the value of $\rho_c N^2 D_I^5$. The viscosity of the continuous phase was in the range of 1.005—4860 centi-poise, and its Reynolds number ranged from 2.63 to 110000. The log-log plot gives roughly the following experimental equation:

$$\log T = \alpha \log(\rho_c N^2 D_I^5) + \beta \tag{9}$$

where α is the slope of the straight line and β is the intercept on the ordinate.

From the data of previous reports, it is also quite certain that the agitation torque is approximately proportional to the agitation intensity,[14] $\rho_c N^2 D_I^5$, as obtained above. Table 3 gives the values of α and β calculated from Eq. 9 by the least-squares method. The interrelation coefficients are also listed in the same table. From Fig. 1, it is found that the agitation torque has a slightly higher value over the whole range of agitation

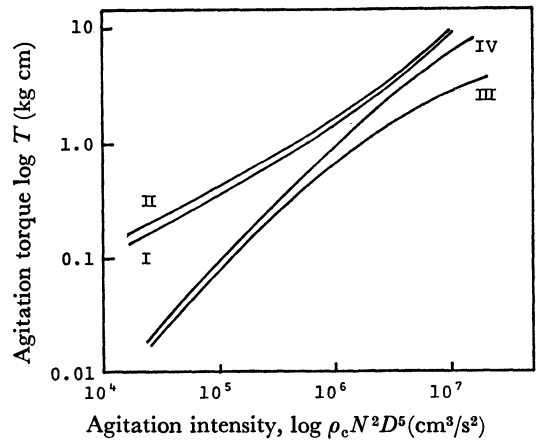

Fig. 1. Relation between agitation torque and agitation intensity at two tank diameters.
I: μ_c=4860 C.P., D_T=150 mmϕ, II: μ_c=4860 C.P., D_T=250 mmϕ, III: μ_c=1.005 C.P., D_T=150 mmϕ, IV: μ_c=1.005 C.P., D_T=250 mmϕ, Tween-20: 0.1% (w/w).

Table 3. The values of α and β calculated from Eq. 9 and of the interrelation coefficient

Viscosity ratio μ_d/μ_c	Tank diameter D_T (mm)	Slope α	Intercept at $\rho_c N^2 D_I^5=1$ β	Interrelation coefficient
8.36×10^{-1}	150	0.793	−5.003	0.991
	200	0.913	−5.629	0.994
	250	1.004	−6.131	1.000
8.61×10^{-2}	150	0.864	−5.332	0.992
	200	0.957	−5.828	0.997
	250	1.000	−6.065	0.999
8.61×10^{-3}	150	0.920	−5.645	0.998
	200	1.000	−6.085	1.000
	250	0.990	−6.010	0.999
7.77×10^{-4}	150	0.867	−5.194	0.999
	200	0.862	−5.155	0.999
	250	0.863	−5.157	1.000
7.77×10^{-5}	150	0.683	−3.868	0.997
	200	0.668	−3.740	0.997
	250	0.678	−3.788	0.996

intensity in the tank having a larger diameter. Furthermore, the agitation torque increases noticeably with increasing viscosity of the continuous phase, indicating that it is greatly affecting by the viscosity.

Effect of the Impeller Diameter on the Particle Size Distribution. The particle size distributions after 60 min of agitation, calculated from the length diameters of particles at three different impeller diameters, are shown in Fig. 2. At each impeller diameter, the size distribution had only one peak, at a particle size of about 12.5 μm. However, as the impeller diameter became smaller, the size distribution spread over a wider range of 5 to 50 μm.

Figure 3 shows changes in the mean surface-volume diameter of droplets at four impeller diameters and at three different viscosity ratios. At two viscosity ratios, 0.00861: 1 and 0.000173: 1, a plot of the mean surface-volume diameter against the impeller diameter gave

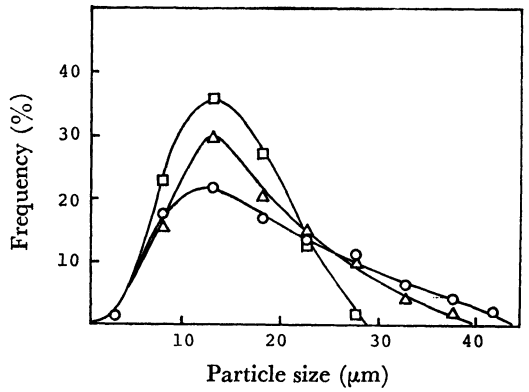

Fig. 2. Particle size distributions at three different impeller diameters.
N: 400 rpm, θ: 60 min, Tween-20: 0.1% (w/w), μ_d/μ_c: 8.61×10^{-3}: 1,
○: D_I=49.0 mm, △: D_I=65.0 mm, □: D_I=89.8 mm.

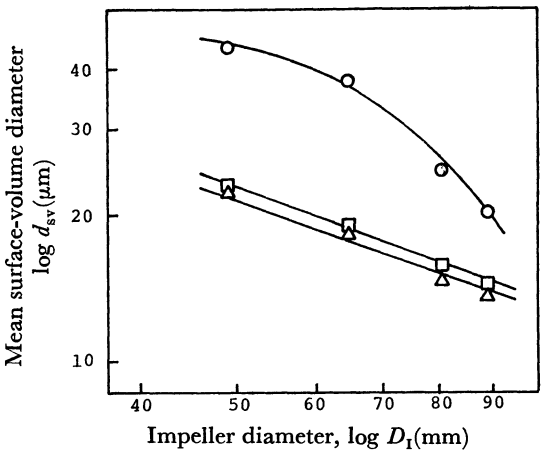

Fig. 3. Relation between mean surface-volume diameter and impeller diameter.
D_T: 150 mmϕ, N: 400 rpm, Tween-20: 0.1% (w/w), ○: μ_d/μ_c=0.836: 1, △: $\mu_d/\mu_c=8.61\times10^{-3}$: 1, □: $\mu_d/\mu_c=1.73\times10^{-4}$: 1.

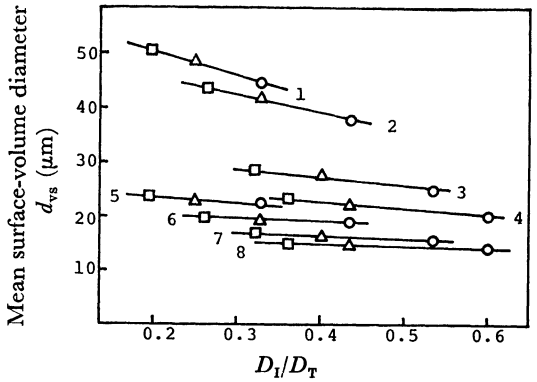

Fig. 4. Relation between mean surface-volume diameter and value of D_I/D_T.
N': 400 rpm, θ: 60 min, Tween-20: 0.1% (w/w).
○: D_T=150 mm, △: D_T=200 mm, □: D_T=250 mm.
1: μ_1, D_I=49.0 mm, 2: μ_1, D_I=65.0 mm, 3: μ_1, D_I=80.1 mm, 4: μ_1, D_I=89.8 mm, 5: μ_5, D_I=49.0 mm, 6: μ_5, D_I=65.0 mm, 7: μ_5, D_I=80.1 mm, 8: μ_5, D_I=89.8 mm.

approximately a straight line, while a convex curve was obtained at 0.836: 1, as illustrated in Fig. 3. The mean surface-volume diameter as measured at the same impeller diameter showed the smallest value when the viscosity ratio was 0.00861: 1. The relation between the mean surface-volume diameter and the diameter ratio of impeller to tank, D_I/D_T, is shown in Fig. 4. It was generally found that the mean surface-volume diameter decreased linearly with increase in the value of D_I/D_T. However, the slope of the straight line became smaller as both the impeller diameter and the viscosity of the continuous phase increased.

Effect of the Revolution Number on the Particle Size Distribution. The particle size distributions calculated by using the length diameters measured at three different revolution numbers are shown in Fig. 5. At each revolution number, the size distribution had only one peak, at a particle size of about 12.5 μm. However, the size distribution took a narrower and sharper shape with increase in the revolution number.

Figure 6 shows the relation between the mean surface-volume diameter of the droplets and the revolution number. When the continuous phase consisted of distilled water (μ_d/μ_c=0.836: 1) alone, a convex curve was observed. On the contrary, when the continuous phase consisted of a mixture of distilled water and sodium silicate (μ_d/μ_c=0.00861: 1 or 0.000173: 1), concave curves could be seen in the figure. In addition, the dependency of the mean surface-volume diameter on the viscosity ratio decreased remarkably at the highest revolution number (N'=812 rpm).

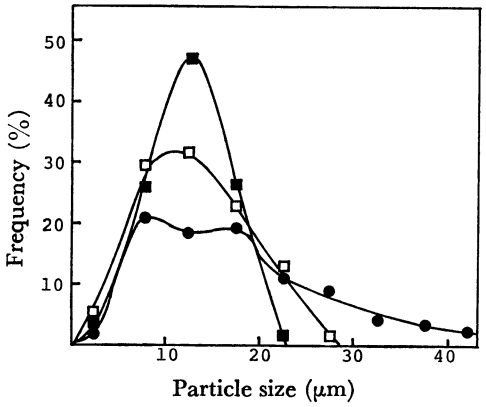

Fig. 5. Particle size distributions at three different revolution numbers.
D_I: 65.0 mm, D_T: 150 mm, θ: 60 min, Tween-20: 0.1% (w/w), $\mu_d/\mu_c=8.61\times10^{-3}$.
●: 330 rpm, □: 660 rpm, ■: 812 rpm.

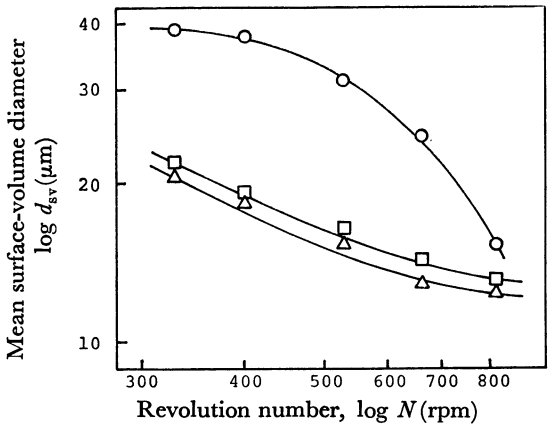

Fig. 6. Relation between mean surface-volume diameter and revolution number.
D_I: 65.0 mm, D_T: 150 mmϕ, Tween-20: 0.1% (w/w).
○: μ_d/μ_c=0.836: 1, △: $\mu_d/\mu_c=8.61\times10^{-3}$: 1, □: $\mu_d/\mu_c=1.73\times10^{-4}$: 1.

Effect of the Viscosity Ratio on the Particle Size Distribution. Changes in the mean surface-volume diameter with viscosity ratio are shown in Fig. 7. At each revolution number, the mean surface-volume diameter increased abruptly as the viscosity ratio approached unity. This tendency was particularly notable at two low revolution numbers, 330 and 400 rpm. On the other hand, the curves had a minimum value at a viscosity ratio of 10^{-2}: 1. In the region where the viscosity ratio is below 10^{-2}: 1, the curves were almost flat.

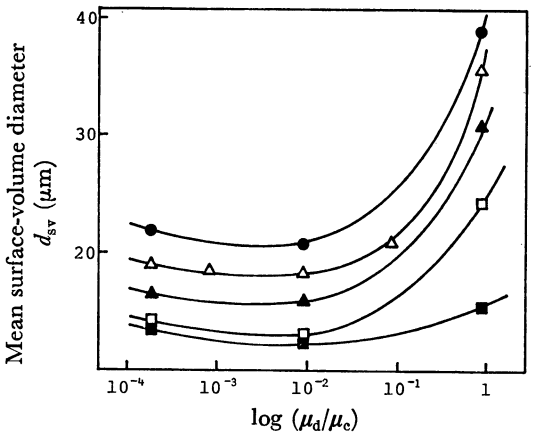

Fig. 7. Relation between mean surface-volume diameter and viscosity ratio.
D_I: 65.0 mm, D_T: 150 mm, θ: 60 min, Tween-20: 0.1% (w/w).
●: 330 rpm, △: 400 rpm, ▲: 530 rpm, □: 660 rpm, ■: 812 rpm.

Energy Efficiency of Agitation in Emulsion. In the present study, the agitation torque, the agitation power, and Reynolds number are as given below:

T: 0.025—8.5 (kgw cm), P: 0.045—73 (watt)

N_{Re}: 2.6—110000 (—)

Under the above conditions, we can now discuss the relation between the energy efficiency of agitation and the agitation conditions in order to obtain a valuable guide for finding the optimum conditions for making emulsions. In this study, the parameters characterizing agitation are chosen to be the viscosity ratio, the mean surface-volume diameter, and the agitation power.

First, the effect of the viscosity ratio on the energy efficiency is shown in Fig. 8. As can be seen from the figure, the relation gave a convex curve at each revolution number and each of the curves had a maximum value near μ_d/μ_c=0.00861: 1, except for the case of the high revolution number of 812 rpm. This means that the agitation power increases and, therefore, the agitation energy becomes higher as the viscosity of the conti-

nuous phase rises. On the other hand, the cohesion and coalescence of droplets during the agitation are obstructed by the high viscosity of the continuous phase, since subdivision of droplets occurs frequently and easily. Accordingly, when the viscosity ratio aproaches 0.00861: 1, the agitation energy and the interfacial energy are balanced.

Secondly, Fig. 9 shows the relation between the mean surface-volume diameter and the energy efficiency. It was found that the value of energy efficiency (μ_d/μ_c= 0.00861: 1 and 0.000173: 1) decreased linearly as the mean surface-volume diameter became smaller, while a concave curve was obtained at a viscosity ratio of 0.836: 1. This tendency can be interpreted as follows. For large droplets, break-up may be possible by only weak shear forces of agitation, while in small ones break-up may be impossible unless the droplets are subjected to strong shear forces of agitation. Thus, the probability for small droplets to burst may be low.

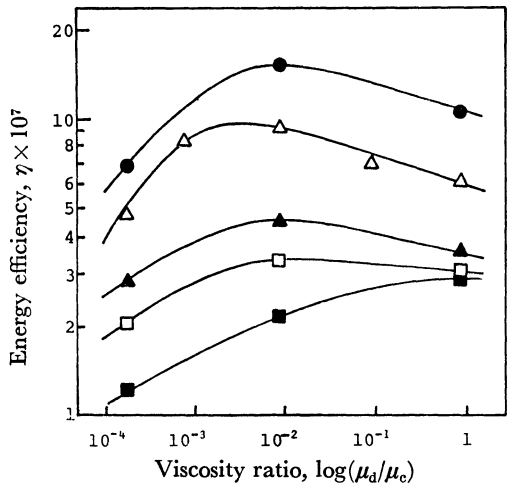

Fig. 8. Relation between energy efficiency and viscosity ratio.
D_I: 65.0 mm, D_T: 150 mmϕ, θ: 60 min, Tween-20: 0.1% (w/w).
●: 300 rpm, △: 400 rpm, ▲: 530 rpm, □: 660 rpm, ■: 812 rpm.

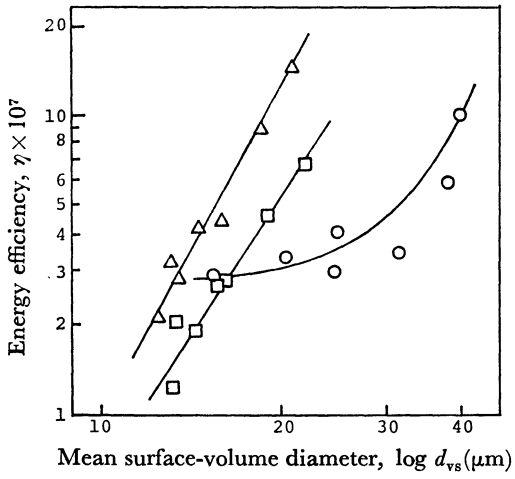

Fig. 9. Relation between energy efficiency and mean surface-volume diameter.
D_I: 65.0 mm, D_T: 150 mmϕ, θ: 60 min, Tween-20: 0.1% (w/w).
○: μ_d/μ_c=0.836: 1, △: $\mu_d/\mu_c=8.61\times10^{-3}$: 1, □: $\mu_d/\mu_c=1.73\times10^{-4}$: 1.

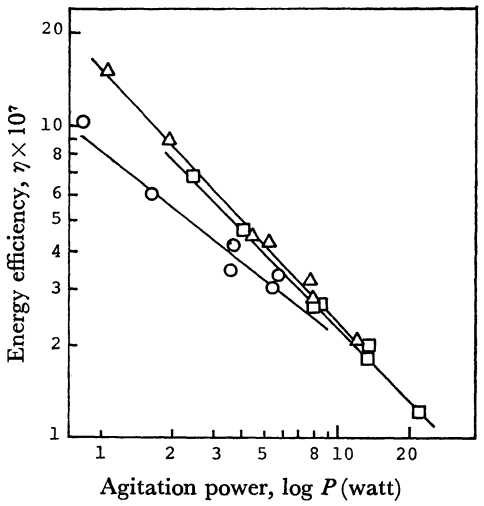

Fig. 10. Relation between energy efficiency and agitation power.
D_I: 65.0 mm, D_T: 150 mmϕ, θ: 60 min, Tween-20: 0.1% (w/w).
○: μ_d/μ_c=0.836: 1, △: $\mu_d/\mu_c=8.61\times10^{-3}$: 1, □: $\mu_d/\mu_c=1.73\times10^{-4}$: 1.

Finally, the relation between the energy efficiency and agitation power is shown in Fig. 10. The agitation power ranged from 1 to 20 watts. The energy efficiency decreased linearly as the agitation power increased. Thus, it is preferable to use as low an agitation power as possible in the formation of emulsions. In addition, the energy efficiency increased in the order of the viscosity ratios, μ_d/μ_c=0.00861: 1>μ_d/μ_c=0.000173: 1>μ_d/μ_c= 0.836: 1. Consequently, the effect of increasing the viscosity ratio is to decrease the rate of cohesion of the droplets, thereby raising the stability of the emulsions.

References

1) J. P. Ward and J. G. Knudsen, *AIChE J.*, **13**, 356 (1967).
2) A. A. Farugui, J. W. Finningan, C. H. Wright, and J. G. Knudsen, *AIChE J.*, **8**, 335 (1962).
3) P. Sherman, "Emulsion Science," Academic Press, New York (1968), p. 21.
4) S. V. Subramanyam and E. S. R. Gopal, *Ind. J. Technol.*, **5**, 139 (1968).
5) J. H. Rushton, E. W. Costich, and H. J. Everett, *Chem. Eng. Progr.*, **46**, 395 (1950).
6) T. Sasaki, *Kagaku Kogaku*, **31**, 432 (1967).
7) S. Tsukiyama and A. Takamura, *Chem. Pharm. Bull.*, **22**, 2607 (1974).
8) S. Tsukiyama, H. Takahashi, I. Takashima, and S. Hatano, *Yakugaku Zasshi*, **91**, 305 (1971).
9) S. Tsukiyama, A. Takamura, Y. Wakamatsu, and I. Takashima, *Yakugaku Zasshi*, **93**, 191 (1973).
10) M. Shigeta, T. Hayakawa, and S. Fujita, *Kagaku Kogaku*, **36**, 211 (1972).
11) S. Tsukiyama, A. Takamura, Y. Fukuda, and M. Koishi, *Bull. Chem. Soc. Jpn.*, **48**, 3561 (1975).
12) J. H. Rushton, D. E. Mack, and H. J. Everett, *Trans. Am. Inst. Chem. Engrs.*, **42**, 441 (1946).
13) S. Nagata, *Chem. Eng.*, **18**, 228 (1954).
14) S. Tsukiyama and A. Takamura, *Chem. Pharm. Bull.*, **23**, 616 (1975).